

# A Positive Charge at Position 33 of Thioredoxin Primarily Affects Its Interaction with Other Proteins but Not Redox Potential<sup>†</sup>

Tiao-Yin Lin\* and Ton-Seng Chen

Department of Biological Science and Technology, National Chiao Tung University, Hsinchu, Taiwan, Republic of China

Received August 24, 2003; Revised Manuscript Received October 14, 2003

**ABSTRACT:** Oxidoreductases of the thioredoxin superfamily possess the C-X-X-C motif. The redox potentials vary over a wide range for these proteins. A crucial determinant of the redox potential has been attributed to the variation of the X-X dipeptide. Here, we substitute Lys for Gly at the first X of *Escherichia coli* thioredoxin to investigate how a positive charge would affect the redox potential. The substitution does not affect the protein's redox potential. The equilibrium constant obtained from pairwise reaction between the mutant and wild-type proteins equals 1.1, indicating that the replacement does not significantly affect the thiol–disulfide redox equilibrium. However, the catalytic efficiency of thioredoxin reductase on the G33K mutant decreases approximately 2.8 times compared to that of the wild type. The mutation mainly affects  $K_m$ , with little effect on  $k_{cat}$ . The mutation also inhibits thioredoxin's ability to reduce insulin disulfide by approximately one-half. Whether the mutant protein supports the growth of phages T3/7 and f1 was tested. The efficiency of plating (EOP) of T3/7 on the mutant strain decreases 5 times at 37 °C and  $3 \times 10^4$  times at 42 °C relative to that of the wild-type strain, suggesting that interaction between phage gene 5 protein and thioredoxin is hindered. The mutation also reduces the EOP of phage f1 by 8-fold at 37 °C and 1.5-fold at 42 °C. The global structure of the mutant protein does not change when studied by CD and fluorescence spectra. Therefore, G33K does not significantly affect the overall structure or redox potential of thioredoxin, but primarily interferes with its interaction with other proteins. Together with the G33D mutation, the overall results show that a charged residue at the first X has a greater influence on the molecular interaction of the protein than the redox potential.

Thioredoxin is a small ( $M_r \sim 12\,000$ ) disulfide-containing redox protein. It is a member of the ubiquitous thiol–disulfide oxidoreductase family. Thioredoxin serves as a hydrogen donor for a wide variety of proteins, such as ribonucleotide reductase (1) and methionine sulfoxide reductase (2, 3). Its function as a general protein disulfide reductase has also been demonstrated in the case of insulin (4). Thioredoxin is involved in numerous cellular processes (5–8), including activation of the glucocorticoid receptor (9, 10) and several chloroplast enzymes (11–13) and modulation of transcription factors such as nuclear factor  $\kappa$ B (NF- $\kappa$ B)<sup>1</sup> and activator protein-1 (AP-1) (14). The protein regulates growth and death of cells, and may be associated with a number of human diseases (see ref 8 for a review).

The three-dimensional structure of the oxidized *Escherichia coli* thioredoxin has been determined by X-ray crystallography (15, 16). The structure of reduced thioredoxin has

been determined by NMR (17–19). Thioredoxin consists of a central five-stranded  $\beta$ -sheet flanked by four helices. Reduced and oxidized forms exhibit almost identical tertiary folds, except for subtle conformational changes in the vicinity of the active site region and the loops that contact it (17–19). The active site is located in a protrusion at the end of the second  $\beta$ -strand and followed by the second  $\alpha$ -helix. The catalytic disulfide of thioredoxin is composed of residues Cys32, Gly33, Pro34, and Cys35.

In addition to the redox activity, *E. coli* thioredoxin is required for growth of several bacteriophages. It is a constituent of T7 phage DNA polymerase. It forms a 1:1 complex with gene 5 protein of T7 phage, and confers high processivity on the DNA polymerase (20, 21). Thioredoxin also takes part in the assembly of filamentous phages f1 and M13 (22, 23). The active site of thioredoxin was thought to be part of the protein surface interacting with the f1 phage assembly machinery (24). Mutant thioredoxin with one or both of the active site cysteines changed to Ser or Ala can support nearly normal viral growth for both f1 and T7 (24, 25). Hence, the redox property is not necessary for viral growth.

The members of the thioredoxin superfamily of thiol–disulfide oxidoreductases have redox potentials spanning a wide range. The highly reducing *E. coli* thioredoxin has an  $E^\circ$  of  $-0.27\text{ V}$  (26–28), and the oxidizing *E. coli* Dsb A, a disulfide bridge-forming enzyme, has an  $E^\circ$  of  $-0.09$  to  $-0.124\text{ V}$  (29–31). On the other hand, the eukaryotic protein

<sup>†</sup> This work was supported by National Science Council Research Grants NSC-90-2311-B-009-004 and NSC-91-2311-B-009-005 of Taiwan, Republic of China.

\* To whom correspondence should be addressed: Department of Biological Science and Technology, National Chiao Tung University, 75 Poai St., Hsinchu, Taiwan, Republic of China. Telephone: 886-3-5712121, ext. 56907. Fax: 886-3-5729288. E-mail: tylin@cc.nctu.edu.tw.

<sup>1</sup> Abbreviations: NF- $\kappa$ B, nuclear factor  $\kappa$ B; AP-1, activator protein-1; PDI, protein disulfide isomerase; IPTG, isopropyl  $\beta$ -D-thiogalactopyranoside; PMSF, phenylmethanesulfonyl fluoride; PCR, polymerase chain reaction; DTNB, 5,5'-dithiobis(2-nitrobenzoic acid); SDS, sodium dodecyl sulfate; PAGE, polyacrylamide gel electrophoresis; DTT, dithiothreitol; CD, circular dichroism; EOP, efficiency of plating.

disulfide isomerase (PDI) has an intermediate  $E^{\circ'}$  of  $-0.147$  to  $-0.175$  V (32, 33). Like thioredoxin, the C-X-X-C motif is essential for the redox function of these enzymes. Alteration of the X-X dipeptide perturbs the reduction potential in the order of the related natural enzymes. For instance, thioredoxin mimicking the active site sequence of PDI results in a 35 mV increase in redox potential (28). A mutation in one of the domains of PDI to the active site sequence of thioredoxin decreases the  $E^{\circ'}$  by 70 mV (34). Changing the X-X residues of the C-X-X-C motif in thioredoxin to the DsbA sequence results in a reductant that is 66 mV less potent (35), while changing the X-X dipeptide of DsbA to that of thioredoxin yields an oxidant that is approximately 90 mV less potent (36).

Through the above and other mutagenesis studies, it has commonly been thought that the sequences of X-X dipeptides are a determinant for the redox potential of the thioredoxin superfamily of oxidoreductases (37). However, it has been shown that mutation of the first X in the active site of thioredoxin to a negatively charged residue (G33D) does not markedly change the redox potential of the protein (38). On the other hand, it influences the kinetics of the reaction with thioredoxin reductase. The mutation also inhibits the function of thioredoxin when it serves as a hydrogen donor for methionine sulfoxide reductase in an *in vivo* study. In the study presented here, we further investigate the problem of the charge effect on the thiol-disulfide oxidoreductase. To gain insights into the effect of the first X on redox potential, a positively charged amino acid, Lys, was substituted for Gly at this position of *E. coli* thioredoxin. We demonstrate that the Gly  $\rightarrow$  Lys substitution, as in the case of the Gly  $\rightarrow$  Asp replacement, does not substantially alter the redox potential or structure of the protein. However, the charged residues significantly affect the redox as well as nonredox functions of thioredoxin. This is achieved mainly by changing thioredoxin's interactions with other proteins rather than by varying the redox potential of the protein.

## EXPERIMENTAL PROCEDURES

**Materials.** The restriction enzymes and T4 DNA ligase were purchased from New England Biolabs Inc. (Beverly, MA) and Promega Corp. (Madison, WI). Bovine insulin was purchased from Sigma Chemical Co. (St. Louis, MO). DNA sequencing was performed with a Perkin-Elmer 377 DNA autosequencer using an ABI Prism Dye Terminator Cycle Sequencing Ready Reaction Kit (PE Applied Biosystems, Foster City, CA).

**Bacterial Strains and Bacteriophage.** *E. coli* strains A179 [HfrC( $\lambda$ )*trxA::kan*] and A179 (pGP1-3), which can express T7 RNA polymerase, were generously provided by S. Tabor (Harvard Medical School, Boston, MA). S. R. Kushner (University of Georgia, Athens, GA) generously supplied *E. coli* SK3981. M. Russel (Rockefeller University, New York, NY) kindly provided *E. coli* A278/pPMR14 carrying a *trxB* gene, and bacteriophage T3/7.

**Construction of pET/G33K Expression Plasmids.** The pET/Trx plasmid contains a *trxA* gene encoding the wild-type thioredoxin. This plasmid was used as a template to generate the G33K mutation by sequential PCRs. In the first PCR, the 5' primer was 5'-TG<sup>GGT</sup>GCAAGCCGTGCAAAATGATC-3' (underlined is the position of nucleotide substitu-

tion), and the 3' primer was 5'-TGATGGTGCATAAGGCCTGAACCAGATCAG-3', which contains a *StuI* site. The nucleotide fragment that was obtained and the T7 primer (5'-TAATACGACTCACTATAGGG-3') were used as 3' and 5' primers, respectively, for the second PCR. The reaction product was cloned to a pGEM-T-easy vector. After transformation of *E. coli* strain DH5 $\alpha$  and selection of white colonies on LB/Amp plates containing X-gal, the plasmid was then purified. The insert was cut from the plasmid by *XbaI* and *EcoRI*, and ligated to the large fragment of pET/Trx that had been treated with the same restriction enzymes to yield the plasmid encoding the G33K mutant thioredoxin (pET/G33K). The mutant gene was confirmed by nucleotide sequencing using a Perkin-Elmer 377 DNA autosequencer. Transformation of *E. coli* strain A179 (pGP1-3) with pET/Trx and pET/G33K yielded A179 (pGP1-3, Trx) and A179 (pGP1-3, G33K), respectively.

**Purification of Thioredoxin.** Expression and purification of proteins are based on the previous protocols (38). Briefly, the culture of A179 (pGP1-3, G33K) was induced with 0.4 mM isopropyl  $\beta$ -D-thiogalactopyranoside (IPTG) at an OD<sub>600</sub> of 0.8, followed by growth at 37 °C for 10 min, switched to 42 °C for 20 min, and then returned to 37 °C for 3 h. Bacteria were then harvested. The pellet was resuspended in 0.05 M Tris and 1 mM EDTA (pH 7.5) (buffer A) with 1 mM phenylmethanesulfonyl fluoride (PMSF) and then sonicated to obtain the crude extract. The crude extract was heated to 80 °C for 5 min and centrifuged to obtain the supernatant. It was treated with 77% ammonium sulfate, and the pellet was dissolved in 15 mL of buffer A. Streptomycin sulfate was added to the solution to yield a final concentration of 0.7% (w/v), and the supernatant was collected after centrifugation. The supernatant was dialyzed against buffer A, applied to a DEAE column, and eluted with a gradient of NaCl. The fractions were checked by the absorbance at 280 nm and SDS-polyacrylamide gel electrophoresis (SDS-PAGE). Fractions containing thioredoxin were further purified on a G-50 gel filtration column. The column was eluted with buffer A. The thioredoxin peak, as checked by the absorbance at 280 nm and SDS-PAGE, was collected. Thioredoxin, thus purified, yielded a single band on SDS-PAGE. Wild-type thioredoxin was purified from *E. coli* SK3981 following the above purification procedures without induction.

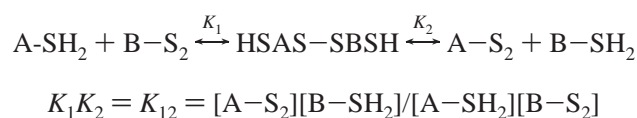
**Electrophoresis.** SDS-PAGE analysis of reduced and denatured proteins was performed in a 10 to 15% SDS-PAGE gel as described by Laemmli (39). The gel was stained with Coomassie blue after electrophoresis. Native gel electrophoresis for the wild-type and mutant thioredoxin was run on a 15% polyacrylamide gel under a nondenaturing condition (40).

**Purification of Thioredoxin Reductase.** Thioredoxin reductase was purified from *E. coli* A278/pPMR14 as described previously (38). Briefly, the culture was grown in LB/ampicillin medium to mid-log phase. Cells were lysed via sonication, and nucleic acids were precipitated with 1.4% streptomycin sulfate. After centrifugation, the supernatant was treated with 82% ammonium sulfate. The precipitate was dissolved, dialyzed against 0.05 M Tris-HCl, 1 mM EDTA, and 0.06 M NaCl (pH 7.4), and applied to a DEAE column equilibrated with the same buffer. The column was developed with a linear gradient from 0.06 to 0.5 M NaCl

in 0.05 M Tris and 1 mM EDTA (pH 7.4). The fractions were checked by the absorbance at 280 nm and SDS-PAGE. They were also tested for activity by the 5,5'-dithiobis(2-nitrobenzoic acid) (DTNB) assay. Peak fractions of thioredoxin reductase were concentrated and applied to a Sephadex G100 column in 0.05 M Tris, 1 mM EDTA, and 0.06 M NaCl (pH 7.4). Then peak fractions of thioredoxin reductase, as checked by SDS-PAGE and the DTNB assay, were rechromatographed on the same column to remove the residual impurity.

**DTNB Assay.** The procedure follows that of Moore *et al.* (26) and Slaby and Holmgren (41). The assay mixture contains 0.1 mg/mL bovine serum albumin, 0.5 mM DTNB, 50–500 nM thioredoxin, 0.24 mM NADPH in a solution of 0.1 M Tris-HCl, and 2 mM EDTA (pH 7.5). The reaction was started by addition of thioredoxin reductase, and the absorbance was followed at 412 nm in a GBC 918 spectrophotometer with an extinction coefficient  $\epsilon_{412}$  of  $13\,600\text{ M}^{-1}\text{ cm}^{-1}$  for thionitrobenzoate (TNB). The kinetics of the reaction were studied by using 0.1–5  $\mu\text{M}$  wild-type or 0.2–7  $\mu\text{M}$  G33K thioredoxin, 3–7 nM thioredoxin reductase, 0.24 mM NADPH, 0.1 mg/mL BSA, 0.5 mM DTNB in 0.1 M sodium phosphate buffer, and 2 mM EDTA (pH 7).

**Redox Equilibrium between Mutant and Wild-Type Thioredoxin.** The method of Aslund *et al.* (42) was used with some modification to measure the redox equilibrium between G33K and wild-type thioredoxin. The reduced wild-type thioredoxin and oxidized G33K thioredoxin were dissolved in 200  $\mu\text{L}$  of an  $\text{N}_2$ -purged solution of 0.1 M sodium phosphate and 1 mM EDTA (pH 7) to concentrations of approximately 5  $\mu\text{M}$ . Reduced wild-type thioredoxin was prepared by reduction of the protein with 10 mM dithiothreitol, followed by Sephadex G25 gel filtration chromatography. The solution was kept under anaerobic conditions overnight at 25 °C, and the sample was quenched with HCl to pH 2. The reduced and oxidized forms of the proteins were separated by reverse phase HPLC on a C18 reverse phase column. The peaks were monitored at 220 nm and quantitated. The apparent concentration equilibrium constant for the thiol–disulfide exchange reaction between the mutant (A) and the wild-type (B) proteins ( $K_{12}$ ) is as follows



The difference in redox potential between the mutant and the wild-type proteins,  $\Delta E^{\circ'}_{\text{AB}}$ , can be obtained using the Nernst equation

$$\Delta E^{\circ'}_{\text{AB}} = E^{\circ'}_{\text{A}} - E^{\circ'}_{\text{B}} = -(RT/nF) \ln K_{12}$$

where  $R$  is the gas constant ( $1.987\text{ cal K}^{-1}\text{ mol}^{-1}$ ),  $n$  is the number of electrons transferred in the reaction, and  $F$  is Faraday's constant ( $23\,040.612\text{ cal mol}^{-1}\text{ V}^{-1}$ ).

**Insulin Disulfide Reduction by the NADPH Coupled Assay.** Insulin disulfide reduction was assessed by the NADPH coupled assay (43, 44). The assay mixture consists of 80  $\mu\text{M}$  insulin, 0.4 mM NADPH, 0.2  $\mu\text{M}$  G33K or wild-type thioredoxin in 0.1 M sodium phosphate, and 2 mM EDTA (pH 7). The reaction was started by addition of 150 nM thioredoxin reductase. NADPH consumption was followed

at 340 nm, using a molar extinction coefficient of  $6200\text{ M}^{-1}\text{ cm}^{-1}$ . To measure the amount of reduced insulin disulfide, 100  $\mu\text{L}$  of the assay mixture prepared as described above was incubated at 25 °C for 30 min, and the reaction was stopped by addition of 0.5 mL of 6 M guanidine-HCl and 1 mM DTNB. The total number of SH groups was determined at  $A_{412}$ , using an extinction coefficient of  $13\,600\text{ M}^{-1}\text{ cm}^{-1}$  for TNB.

**Viability of Phage T3/7.** *E. coli* strain SK3967 carrying pET/G33K was grown in T medium until an  $\text{OD}_{600}$  of 0.5 had been reached and then infected with T3/7 that had been serially diluted. The infected cells were plated on agar plates and incubated at 37 or 42 °C. The efficiency of plating (EOP) was determined with reference to the plaque number obtained on SK3967 (pET/Trx).

**Viability of Phage f1.** *E. coli* strain A179 (pGP1-3) carrying pET/G33K was grown in f1 medium until an  $\text{OD}_{600}$  of 0.5 had been reached and infected with f1 at the appropriate dilution. The infected cells were plated on agar plates and incubated at 37 or 42 °C. The EOP was determined with reference to the plaque number obtained on the same *E. coli* strain harboring the wild-type *trxA* plasmid.

**Circular Dichroism Measurements.** An AVIV model 62 DS spectrophotometer was used to determine the CD spectra of the wild-type and mutant proteins at 25 °C. The far-UV CD measurements were taken at a protein concentration of approximately  $9 \times 10^{-6}\text{ M}$  in 0.05 M sodium phosphate and 0.1 mM EDTA (pH 7.5) using a quartz cell with a path length of 1 mm. The spectra were taken from 190 to 260 nm with a step resolution of 0.5 nm and a bandwidth of 1.0 nm. For the reduced protein, approximately  $6 \times 10^{-5}\text{ M}$  protein was first reduced by DTT at a concentration  $\sim 10$  times higher. The solution was then diluted to the final protein concentration for measurements.

**Fluorescence Measurements.** A thermostated Hitachi F-4500 spectrofluorimeter was used to determine the fluorescence spectra of wild-type and mutant thioredoxin at 25 °C. The excitation wavelength was 280 nm. The bandwidth was 5 nm for both excitation and emission. The measurements were performed at approximately 7  $\mu\text{M}$  thioredoxin in 1 mL of 50 mM sodium phosphate (pH 7.5). To obtain the reduced thioredoxin, 0.4 mM protein was reduced with 8 mM DTT. The reduced samples were diluted to 7  $\mu\text{M}$  for measurements. Solvent blanks were subtracted from the sample spectra.

## RESULTS

**Mutagenesis and Purification of G33K Mutant Thioredoxin.** Thioredoxin is the primordial protein of the thioredoxin superfamily of oxidoreductase. The first X in the active site of thioredoxin is a conserved Gly33. It was mutated to Lys by site-directed mutagenesis. An oligonucleotide containing one base mismatch for producing the Gly33  $\rightarrow$  Lys mutation was used as the primer in the PCR. The mutation was later confirmed by sequencing the entire gene. The mutant as well as the wild-type proteins were expressed and purified by DEAE ion exchange and G50 gel filtration chromatography. The purified G33K and the wild-type thioredoxin migrated on an SDS-PAGE gel as single bands of 12 kDa (Figure 1A). When an excessive amount of the G33K mutant protein was loaded onto a native polyacryla-



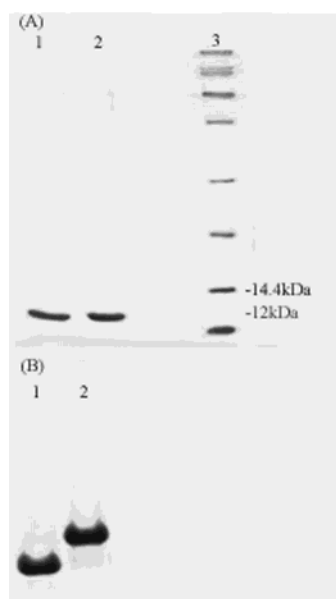


FIGURE 1: (A) SDS-15% polyacrylamide gel electrophoresis of G33K and wild-type thioredoxin: 2  $\mu$ g of wild-type thioredoxin (lane 1) and 2  $\mu$ g of G33K thioredoxin (lane 2). (B) Native 15% polyacrylamide gel electrophoresis of G33K and wild-type thioredoxin: 11  $\mu$ g of wild-type protein (lane 1) and 16  $\mu$ g of G33K protein (lane 2).

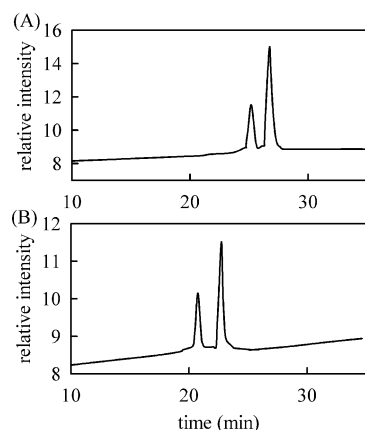


FIGURE 2: HPLC analysis of oxidized and reduced G33K thioredoxin. Purified G33K thioredoxin was injected into a reverse phase HPLC column and monitored at 220 nm. The protein was eluted with an acetonitrile gradient first from 27 to 38.7% over the course of 10 min and then from 38.7 to 58.5% over an additional 27 min: (A) 10  $\mu$ g of oxidized G33K thioredoxin and (B) 10  $\mu$ g of G33K thioredoxin reduced with 2 mM DTT.

mide gel and electrophoresis was carried out under nonreducing conditions, a single band was observed, again demonstrating that the protein was pure (Figure 1B). Compared to the wild-type protein, the G33K protein ran at a slower rate to the anode, indicating that the isoelectric point of the G33K mutant had increased (Figure 1B).

**HPLC Analysis of the G33K Protein.** The G33K mutant protein purified as described above was subjected to reverse phase HPLC to investigate the conversion between the oxidized and reduced forms of the protein. The oxidized protein (Figure 2A) was converted to the reduced form when reduced by DTT (Figure 2B). However, besides the main peak, a smaller peak was also found in the chromatogram in both the reduced and oxidized forms. The smaller peak, herein called G33K\*, appears to closely resemble the main

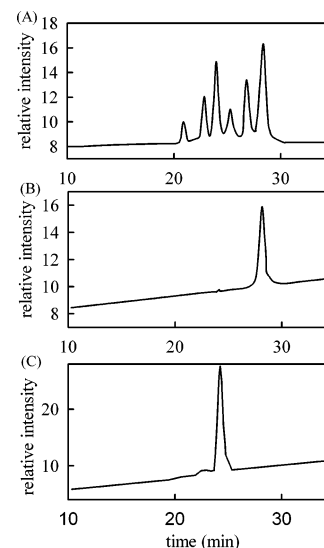


FIGURE 3: HPLC analysis of the redox equilibrium between G33K and wild-type thioredoxin. (A) Reduced wild-type thioredoxin (4.4  $\mu$ M, 10.4  $\mu$ g) and oxidized G33K thioredoxin (4.1  $\mu$ M, 9.8  $\mu$ g) were incubated in 0.1 M phosphate and 1 mM EDTA (pH 7) for 15 h, and then the reaction was quenched with HCl before HPLC analysis. (B) Oxidized wild-type thioredoxin (5.4  $\mu$ g). (C) Reduced wild-type thioredoxin (11.2  $\mu$ g). Positions of oxidized and reduced G33K thioredoxin are as shown in Figure 3.

Table 1: Ratio of Redox Equilibria between the Mutant and Wild-Type Thioredoxin at pH 7

thioredoxin	$K_{\text{mutant}}/K_{\text{wt}}$	$\Delta E^{\circ'}$ (mV)	$E^{\circ'}$ (mV)
wild-type			-270
G33K	$1.1 \pm 0.1$	-1.2	-271
G33K*	$1.1 \pm 0.1$	-1.2	-271
G33D	$0.8 \pm 0.1$	2.9	-267

peak in all the purification steps and electrophoresis analysis. The fact that G33K\* was also reduced by DTT further strengthened this point. The existence of this additional peak does not interfere with the properties of the protein (see below). An additional peak after purification of thioredoxin has also been reported in the literature (42, 45, 46).

**Redox Equilibrium between the G33K and Wild-Type Proteins.** The difference in redox potential between two proteins can be determined by direct protein-protein equilibration. The reduced and oxidized forms of the wild-type and mutant proteins were separated by HPLC as shown in Figure 3 for the G33K mutant. The ratio of redox equilibrium constants between the G33K and wild-type proteins was 1.1 at pH 7 (Table 1). Therefore, a positive charge at position 33 has little effect on the redox potential of the protein. The redox equilibrium of G33D and the wild-type protein was also determined by this method. Table 1 shows that it is approximately 0.8. In addition, G33K\* exhibited a ratio of redox equilibrium constants identical to that of G33K.

**Kinetics of the Thioredoxin Reductase-Catalyzed Redox Reaction.** *E. coli* thioredoxin reductase catalyzes the electron transfer between NADPH and thioredoxin. Kinetic parameters of this reaction when using wild-type and G33K mutant proteins as electron acceptors were studied. The G33K substitution did not significantly affect  $k_{\text{cat}}$ , whereas it increased  $K_m$  by 2.5-fold. The catalytic efficiency decreased approximately 2.8-fold compared to that of the wild-type protein (Table 2). Since the kinetic data fit well into the

Table 2: Kinetic Parameters of the Reaction of Thioredoxin Reductase with Thioredoxin at pH 7 and 25 °C

thioredoxin	$k_{\text{cat}}$ ( $\text{min}^{-1}$ )	$K_m$ ( $\mu\text{M}$ )	$k_{\text{cat}}/K_m$ ( $\mu\text{M}^{-1} \text{min}^{-1}$ )
G33K	$1070 \pm 200$	$3.6 \pm 0.3$	297
wild-type	$1250 \pm 100$	$1.5 \pm 0.1$	833

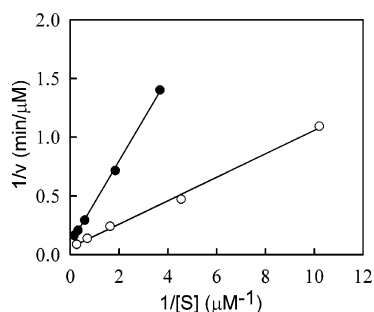


FIGURE 4: Kinetics of wild-type and G33K mutant thioredoxin as substrates in the reaction catalyzed by thioredoxin reductase. The assay condition is described in Experimental Procedures. Thioredoxin reductase concentrations were 5.8 and 6.0 nM for the reaction with the G33K mutant and the wild type, respectively: (●) G33K thioredoxin and (○) wild-type thioredoxin.

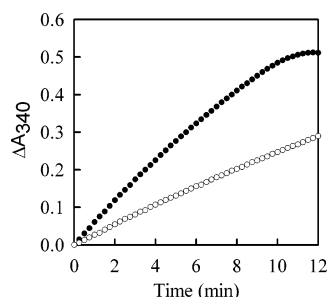


FIGURE 5: Time course of the reduction of insulin by G33K thioredoxin. Insulin (80  $\mu\text{M}$ ) was reduced with 0.2  $\mu\text{M}$  G33K (○) or wild-type (●) thioredoxin at pH 7 in the presence of NADPH. The reaction was started by addition of 150 nM thioredoxin reductase and followed by the absorbance change at 340 nm.

Lineweaver–Burk equation over a 24-fold concentration range (Figure 4), it can also be concluded that the existence of G33K\* does not affect the kinetics of the thioredoxin reductase reaction.

**Reduction of Insulin Disulfide by Reduced G33K Thioredoxin.** Reduction of insulin disulfide was assessed with an assay coupled to the NADPH reduction. As shown in Figure 5, the rate of NADPH consumption was lower by approximately one-half for the G33K mutant than for the wild-type thioredoxin. Insulin precipitation for the wild type occurred after reaction for 12 min, and by that time, 82  $\mu\text{M}$  disulfide had been reduced. Precipitation took place after 19 min for the G33K mutant, and by that time, 64  $\mu\text{M}$  disulfide had been reduced. The total amount of disulfide reduced was measured with the DTNB assay. After reaction for 30 min, approximately 119  $\mu\text{M}$  disulfide was reduced by wild-type thioredoxin, whereas 70  $\mu\text{M}$  disulfide was reduced by the G33K mutant protein (Table 3). Therefore, the mutant protein had ~59% of the activity of the wild type in the reduction of insulin.

**Viability of T3/7 Phages on the G33K Mutant.** *E. coli* thioredoxin is required for the growth of bacteriophage T3/7. Thioredoxin constitutes an essential subunit of the phage DNA polymerase. The ability of G33K thioredoxin to support

Table 3: Activity of G33K and Wild-Type Thioredoxin in the Reduction of Insulin Disulfide at 25 °C and pH 7

thioredoxin	NADPH consumption ( $\mu\text{M}/\text{min}$ )	total disulfide reduced in 30 min ( $\mu\text{M}$ )	activity of thioredoxin (%)
wild-type	9.4	$119 \pm 24$	100
G33K	4.4	$70 \pm 10$	59

Table 4: Efficiency of the Growth of Bacteriophages T3/7 and f1 on *E. coli* Strains<sup>a</sup> Carrying the G33K Mutant or Wild-Type Thioredoxin

thioredoxin	EOP			
	T3/7		f1	
	37 °C	42 °C	37 °C	42 °C
wild-type	1	1	1	1
G33K	$0.20 \pm 0.03$	$(3.2 \pm 2.2) \times 10^{-5}$	$0.12 \pm 0.05$	$0.67 \pm 0.13$

<sup>a</sup> Bacterial strains used for T3/7 and f1 infection were SK3967 and A179(pGP1-3), respectively.

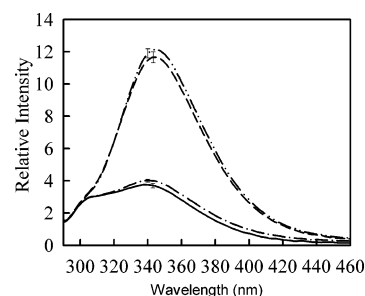


FIGURE 6: Fluorescence spectra of the reduced and oxidized G33K: (—) 7  $\mu\text{M}$  oxidized wild-type thioredoxin, (---) 7  $\mu\text{M}$  oxidized G33K, (···) 7  $\mu\text{M}$  reduced thioredoxin, and (-·-·) 7  $\mu\text{M}$  reduced G33K. The error bars indicate the range of three measurements.

phage T3/7 growth was determined relative to that of the wild-type protein. At 37 °C, the mutation decreased the EOP of T3/7 by 5-fold, indicating that a positive charge at the active site of thioredoxin is unfavorable for the association with gene 5 protein of the phage. At 42 °C, the EOP of T3/7 on the G33K mutant was reduced to  $3.2 \times 10^{-5}$ , suggesting that the complex of gene 5 protein and the mutant thioredoxin is thermosensitive.

**Viability of f1 Phages on the G33K Mutant.** Thioredoxin is necessary for growth of filamentous phage f1. The effects of the G33K mutation on thioredoxin phage f1 growth were determined relative to the wild-type protein. The mutation reduced the EOP by 8- and 1.5-fold at 37 and 42 °C, respectively. The results suggest that a positive charge at the active site of thioredoxin significantly affects the phage assembly.

**Structure of G33K Mutant Thioredoxin.** The structure of G33K thioredoxin was studied by CD and fluorescence spectrometry at pH 7.5. In the far-UV region, oxidized mutant and wild-type thioredoxin exhibit practically the same CD spectra. Their reduced forms also do not exhibit any difference in the far-UV CD spectra (data not shown). Therefore, the secondary structure is not affected by the Gly  $\rightarrow$  Lys substitution. The fluorescence spectra of G33K and wild-type thioredoxin exhibited an emission maximum of 341 nm when fluorescence was excited at 280 nm (Figure 6). The fluorescence increased ~3.5-fold, and the emission

maximum shifted to 345 nm upon reduction for both G33K mutant and wild-type proteins. The observed similarities of the oxidized and the reduced fluorescence spectra of the G33K and wild-type proteins suggest that the tertiary structure of thioredoxin is not significantly changed by the mutation.

## DISCUSSION

Thioredoxin is an electron transport protein that takes part in many cellular oxidation–reduction reactions. The C-X-X-C motif in its active site is essential in carrying out the redox functions. The central residues in the motif are considered to be important in modulating the redox potential. In this paper, we performed a Gly  $\rightarrow$  Lys substitution at the first X position of *E. coli* thioredoxin. Despite the multiple purification steps, the highly purified G33K mutant contains a small amount of G33K\*. The amount of G33K\* varied with different preparations. We have obtained a preparation that has a much smaller amount of G33K ( $\sim 10\%$ ). A single band in SDS–PAGE suggests that it has a molecular mass similar to that of G33K. A single band in the native gel shows that it has the same charge as G33K. G33K\* can be converted between the oxidized and reduced forms, and possesses the same redox potential as the G33K mutant. The practically indistinguishable CD and fluorescence spectra of the G33K and wild-type proteins, in either the oxidized or reduced state, indicate the same folding of this species as G33K protein. The kinetic data of thioredoxin reductase-catalyzed reduction of thioredoxin also suggest that G33K\* does not influence the kinetics of experiments. Therefore, the existence of the additional peak does not interfere with our studies. The presence of two different species in human thioredoxin has been reported, and human thioredoxin was shown to be a protein with or without a methionine at the N-terminus (45, 46). A methionine-containing isoform has also been reported for a mutant of *E. coli* thioredoxin (42).

The redox equilibrium between the G33K mutant and the wild-type protein yields a  $K_{12}$  value of 1.1 at pH 7, corresponding to a  $\Delta E^\circ$  of  $-1.2$  mV. This reveals that G33K does not significantly affect the redox potential of the protein. Using the same method, the direct redox equilibrium between the G33D mutant and the wild-type protein gives a  $K_{12}$  value of 0.8, which is consistent with the ratio of 0.88 taken from the previous reported values of  $C_{\text{eff}}$  (38). The difference of 2.9 mV in the redox potentials between G33D and wild-type thioredoxin obtained in this study also agrees with the value of 3 mV acquired from the investigation of the redox reaction catalyzed by thioredoxin reductase (38). The mutual consistency validates these results of redox potential obtained using direct redox equilibrium. Collectively, these results indicate that a positively charged Lys or negatively charged Asp at the first X of the C-X-X-C motif does not have substantial effects on the redox potential. The positive or negative charge does not interfere with the thiol–disulfide equilibrium, suggesting that the side chain is positioned away from the thiol groups. This point is corroborated by the results of the interaction between the mutant protein and a variety of proteins as discussed below.

Although the redox potential of the G33K mutant does not change significantly, the redox reactions of thioredoxin are, however, affected by the substitution. G33K mutant

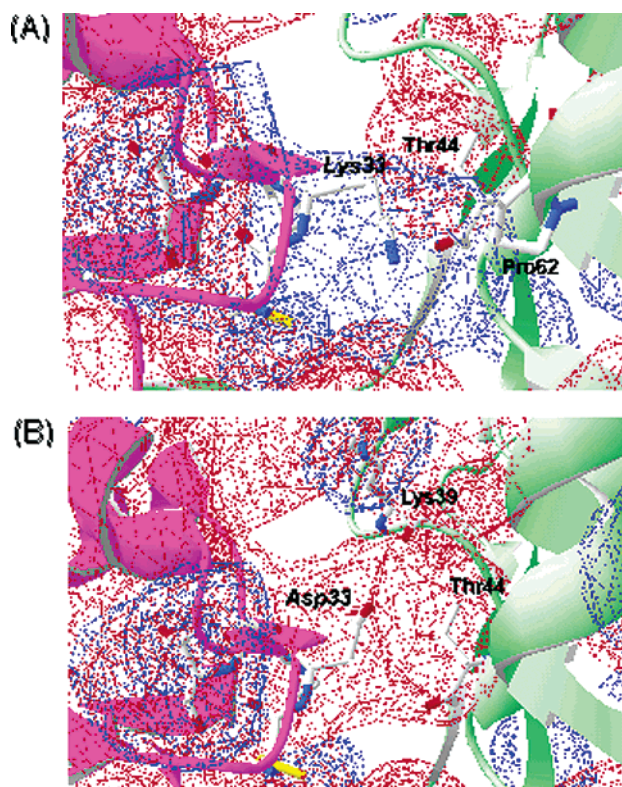


FIGURE 7: Structure of thioredoxin and the thioredoxin reductase complex in the active site region of thioredoxin: (A) G33K thioredoxin and (B) G33D thioredoxin. The modeling was based on the structure of the wild-type thioredoxin–thioredoxin reductase complex (48), and the mutation was refined by energy minimization with GROMOS96 (50). The structural change was confined to the position of mutation. The electrostatic potential map was calculated using formal charges. Models were rendered with SwissPDB Viewer (51). Side chains are drawn for only active site residues of thioredoxin (purple) and residues of thioredoxin reductase (green) that interact with mutated amino acids.

thioredoxin is not an efficient substrate for *E. coli* thioredoxin reductase compared to the wild-type protein. The catalytic efficiency decreases 2.8-fold for the G33K mutant. The  $k_{\text{cat}}$  value ( $1070 \text{ min}^{-1}$ ) for the mutant is close to that of the wild type ( $1250 \text{ min}^{-1}$ ) and the previously reported wild-type value of  $1365 \text{ min}^{-1}$  (47). However, the  $K_m$  of the G33K mutant protein increases to  $3.6 \mu\text{M}$ , which is 2.4-fold higher than the wild-type value of  $1.5 \mu\text{M}$ . The catalytic efficiency on G33K decreases largely because of an increase in  $K_m$ , suggesting that the side chain of lysine is protruding from the surface of thioredoxin and perturbing the interaction with thioredoxin reductase.

CD and fluorescence studies show that the Gly  $\rightarrow$  Lys replacement does not alter the secondary and tertiary structures of the protein. Since the active site is close to Trp28 and Trp31 of thioredoxin, the resemblance between the G33K fluorescence spectra of both the reduced and oxidized forms and those of the wild type strongly shows that the Lys33 substitution does not significantly affect the protein structure. Therefore, the replacement of Gly33 with Lys primarily affects the kinetics of redox reactions, but not the redox potential and structure of the protein.

The substitution of Asp for Gly at position 33 of thioredoxin decreases the catalytic efficiency by approximately 9-fold, which is attributed to an increase in  $K_m$  (38).



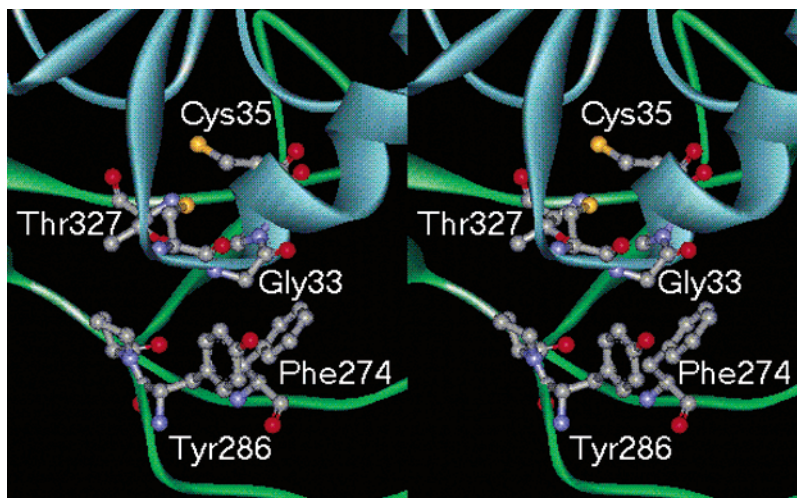


FIGURE 8: Structure of T7 DNA polymerase near Gly33 of thioredoxin. The stereo representation is based on the X-ray crystallography of the thioredoxin–T7 gene 5 protein complex (49). Side chains are shown for only the active site residues of thioredoxin and residues that interact with Gly33 of thioredoxin in the T7 gene 5 protein. Thioredoxin is in blue, and the T7 gene 5 protein is in green. This figure was produced with WebLab Viewer Lite (Accelrys).

Comparison of the catalytic efficiency of thioredoxin reductase on G33K and G33D mutants demonstrates that a negative charge at position 33 is approximately 3 times more unfavorable than a positive charge at the same position. The lower catalytic activity for G33D relative to G33K can be explained by the interaction between thioredoxin and thioredoxin reductase as shown in the models of Figure 7. The models were constructed according to the published X-ray structure of the thioredoxin–thioredoxin reductase complex (48). Because both G33D and G33K were shown to possess the wild-type structure, the changes in these models were confined to substitution sites. Figure 7 shows that both mutations can be adopted without alteration in the other parts of the complex structure. The carboxylic side chain of Asp33 is located in an environment of negative electrostatic potential, close (within 5 Å) to the side chain OG1, the main chain carbonyl of Thr44, and the main chain carbonyl group of Lys39. When lysine is at position 33, the side chain NZ is 7.84 Å from the carbonyl group of Thr44, and the carbons in the side chain are close to Pro62. The more unfavorable electrostatic surroundings of the Asp33 may account for the relatively low catalytic efficiency of thioredoxin reductase compared to Lys33. This provides further support for our point that the charged amino acid at the first X position primarily affects the interaction in the redox reaction.

An arginine has been inserted in the active site of thioredoxin to generate a Cys-Gly-Arg-Pro-Cys sequence (47). The insertion suppresses the ability of thioredoxin to serve as a substrate of thioredoxin reductase. The catalytic efficiency is reduced to  $5 \mu\text{M}^{-1} \text{min}^{-1}$ , which is 137 times lower than that of the wild-type protein. Because the positive charge in G33K has smaller effects on the catalytic efficiency, a large proportion of the decrease in  $k_{\text{cat}}/K_m$  for the Arg insert mutant may result from the expansion of the disulfide ring size. The ring expansion is likely to cause a change in the redox potential. The altered ring size and redox potential, and the presence of a positive charge, altogether can contribute to the severe loss of catalytic efficiency.

Reduction of protein disulfide by the G33K mutant protein was assayed by a thioredoxin reductase-coupled insulin reduction assay with a relatively low concentration of

thioredoxin and a high concentration of thioredoxin reductase. The results demonstrated that G33K thioredoxin is a less efficient protein disulfide reductase with a rate approximately 2-fold lower than that of the wild type. This is consistent with the total amount of disulfide reduced during 30 min of reaction, which showed that the G33K activity is ~59% of that of the wild-type protein. As the redox potential of the G33K protein is the same as the wild-type's potential, the decrease in activity suggests that the side chain of the mutant protein interferes with the interaction of thioredoxin with insulin.

To illustrate further that the first X in the C-X-X-C motif can significantly affect the interaction of thioredoxin with other proteins without evoking a change in the redox potential of the protein, we compared the growth of T3/7 phage supported by the wild-type and the G33K mutant thioredoxin. Substitution of Lys for Gly at the first X reduces the plating efficiency of T3/7, suggesting that the efficiency of DNA polymerase is decreased. X-ray crystallography of the bacteriophage T7 phage DNA replication complex shows that the active site of thioredoxin participates in the interaction with the protein encoded by gene 5 of the phage (49). Substitution of Lys for Gly lowers the growth efficiency by hindering the interaction with the gene 5 protein, which can be inferred from the proximity of position 33 of thioredoxin to Phe274 and Tyr286 of the gene 5 protein (Figure 8). Modeling on the basis of this structure indicates that substitution of Lys for Gly33 would create clashes with the side chain of Phe274. This accounts for the observed 5-fold reduction in the EOP value of phage T3/7 at 37 °C, and its great diminution at 42 °C. The decrease in activity of the G33K thioredoxin in serving as a processivity subunit of phage DNA polymerase indicates a critical role of the first X of the C-X-X-C motif in the protein–protein interaction.

Thioredoxin has been suggested to participate in the interaction with the assembly machinery during the morphogenesis of f1, although the mechanism by which thioredoxin works is not clear. Since the redox activity of thioredoxin is not involved in viral growth (24, 25), the reduced efficiency of growth of f1 in the strain carrying the G33K mutant again suggests that the first X is important in

the interaction of thioredoxin with fl assembly machinery, and a positive charge affects the interaction.

In summary, our study shows that introducing a negative or positive charge at the first X of the C-X-X-C motif of thiol-disulfide oxidoreductase, despite the drastic changes, does not cause a large variation of the redox potential. The substituted charges protrude from the surface to the accessible side of the disulfide bridge. They have more effects on the interaction of thioredoxin with other proteins than on the redox potential.

## ACKNOWLEDGMENT

We gratefully thank Drs. M. Russel, S. Tabor, and S. R. Kushner for gifts of strains and bacteriophage, Dr. P. C. Lyu for lending to us a CD spectrophotometer, and the National Center for High-Performance Computing of ROC for the computing facility.

## REFERENCES

- Laurent, T. C., Moore, E. C., and Reichard, P. (1964) *J. Biol. Chem.* 239, 3436–3444.
- Porque, P. G., Baldesten, A., and Reichard, P. (1970) *J. Biol. Chem.* 245, 2371–2374.
- Ejiri, S.-I., Weissbach, H., and Brot, N. (1980) *Anal. Biochem.* 102, 393–398.
- Holmgren, A. (1979) *J. Biol. Chem.* 254, 9627–9632.
- Holmgren, A. (1985) *Annu. Rev. Biochem.* 54, 237–271.
- Gleason, F. K., and Holmgren, A. (1988) *FEMS Microbiol. Rev.* 54, 271–298.
- Eklund, H., Gleason, F. K., and Holmgren, A. (1991) *Proteins: Struct., Funct., Genet.* 11, 13–28.
- Powis, G., and Monfort, W. R. (2001) *Annu. Rev. Pharmacol. Toxicol.* 41, 261–295.
- Grippio, J. F., Tienrungroj, W., Dahmer, M. K., Housley, P. R., and Pratt, W. B. (1983) *J. Biol. Chem.* 258, 13658–13664.
- Makino, Y., Yoshikawa, N., Okamoto, K., Hirota, K., Yodoi, J., Makino, I., and Tanaka, H. (1999) *J. Biol. Chem.* 274, 3182–3188.
- Buchanan, B. B. (1991) *Arch. Biochem. Biophys.* 288, 1–9.
- Scheibe, R. (1991) *Plant Physiol.* 96, 1–3.
- Balmer, Y., Koller, A., del Val, G., Manierri, W., Schürmann, P., and Buchanan, B. B. (2003) *Proc. Natl. Acad. Sci. U.S.A.* 100, 370–375.
- Schenk, H., Klein, M., Erdbrügger, W., Dröge, W., and Schulze-Osthoff, K. (1994) *Proc. Natl. Acad. Sci. U.S.A.* 91, 1672–1676.
- Holmgren, A., Soderberg, B.-O., Eklund, H., and Holmgren, A. (1975) *Proc. Natl. Acad. Sci. U.S.A.* 72, 2305–2309.
- Katti, S. K., LeMaster, D. M., and Eklund, H. (1990) *J. Mol. Biol.* 212, 167–184.
- Dyson, H. J., Holmgren, A., and Wright, P. E. (1989) *Biochemistry* 28, 7074–7087.
- Dyson, H. J., Gippert, G. P., Case, D. A., Holmgren, A., and Wright, P. E. (1990) *Biochemistry* 29, 4129–4136.
- Jeng, M.-F., Campbell, A. P., Begley, T., Holmgren, A., Case, D. A., Wright, P., and Dyson, H. J. (1994) *Structure* 2, 853–868.
- Mark, D. F., and Richardson, C. C. (1976) *Proc. Natl. Acad. Sci. U.S.A.* 73, 780–784.
- Tabor, S., Huber, H. E., and Richardson, C. C. (1987) *J. Biol. Chem.* 262, 16212–16223.
- Russel, M., and Model, P. (1985) *Proc. Natl. Acad. Sci. U.S.A.* 82, 29–33.
- Lim, C.-J., Haller, B., and Fuchs, J. A. (1985) *J. Bacteriol.* 161, 799–802.
- Russel, M., and Model, P. (1986) *J. Biol. Chem.* 261, 14997–15005.
- Huber, H. E., Russel, M., Model, P., and Richardson, C. C. (1986) *J. Biol. Chem.* 261, 15006–15012.
- Moore, E. C., Reichard, P., and Thelander, L. (1964) *J. Biol. Chem.* 239, 3445–3452.
- Lin, T.-Y., and Kim, P. S. (1989) *Biochemistry* 28, 5282–5287.
- Krause, G., Lundström, J., Lopez-Barea, J. P. C., Pueyo de la Cuesta, C., and Holmgren, A. (1991) *J. Biol. Chem.* 266, 9494–9500.
- Wunderlich, M., and Glockshuber, R. (1993) *Protein Sci.* 2, 717–726.
- Zapun, A., Bardwell, J. C., and Creighton, T. E. (1993) *Biochemistry* 32, 5083–5092.
- Grauschopf, U., Winther, J. R., Korber, P., Zander, T., Dallinger, P., and Bardwell, J. C. A. (1995) *Cell* 83, 947–955.
- Darby, N. J., and Creighton, T. E. (1995) *Biochemistry* 34, 16770–16780.
- Lundström, J., and Holmgren, A. (1993) *Biochemistry* 32, 6649–6655.
- Kortemme, T., Darby, N. J., and Creighton, T. E. (1996) *Biochemistry* 35, 14503–14511.
- Mössner, E., Huber-Wunderlich, M., and Glockshuber, R. (1998) *Protein Sci.* 7, 1233–1244.
- Joelson, T., Sjöberg, B. M., and Eklund, H. (1990) *J. Biol. Chem.* 265, 3183–3188.
- Huber-Wunderlich, M., and Glockshuber, R. (1998) *Folding Des.* 3, 161–171.
- Lin, T.-Y. (1999) *Biochemistry* 38, 15508–15513.
- Laemmli, U. K. (1970) *Nature* 227, 680–685.
- Bollag, D. M., Rozycki, M. D., and Edelstein, S. J. (1996) *Protein Methods*, 2nd ed., pp 155–172, Wiley & Sons, New York.
- Slaby, I., and Holmgren, A. (1979) *Biochemistry* 18, 5584–5591.
- Åslund, F., Berndt, K. D., and Holmgren, A. (1997) *J. Biol. Chem.* 272, 30780–30786.
- Holmgren, A. (1977) *J. Biol. Chem.* 252, 4600–4606.
- Luthman, M., and Holmgren, A. (1982) *Biochemistry* 21, 6628–6633.
- Forman-Kay, J. D., Clore, G. M., Wingfield, P. T., and Gronenborn, A. M. (1991) *Biochemistry* 30, 2685–2698.
- Louis, H. M., Georgescu, R. E., Tasayco, M. L., Tcherkasskaya, O., and Gronenborn, A. M. (2001) *Biochemistry* 40, 11184–11192.
- Gleason, F. K., Lim, C.-J., Maryam, G.-N., and Fuchs, J. A. (1990) *Biochemistry* 29, 3701–3709.
- Lennon, B. W., Williams, C. H., Jr., and Ludwig, M. L. (2000) *Science* 289, 1190–1194.
- Doublé, S., Tabor, S., Long, A. M., Richardson, C. C., and Ellenberger, T. (1998) *Nature* 391, 251–258.
- van Gunsteren, W. F., Billeter, S. R., Eising, A. A., Hünenberger, P. H., Krüger, P., Mark, A. E., Scott, W. R. P., and Tironi, I. G. (1996) *Biomolecular simulation: The GROMOS96 manual and user guide*, Vdf Hochschulverlag AG an der ETH Zürich, Zürich, Switzerland.
- Guex, N., and Peitsch, M. C. (1997) *Electrophoresis* 18, 2714–2723.

BI0355138